European Journal of Medicinal Chemistry 64 (2013) 554–561

Contents lists available at SciVerse ScienceDirect

European Journal of Medicinal Chemistry

journal homepage: http://www.elsevier.com/locate/ejmech

Original article

Platinum(II) complexes containing aminophosphonate esters: Synthesis, characterization, cytotoxicity and action mechanism

Ke-Bin Huang [a,b], Zhen-Feng Chen [b,*], Yan-Cheng Liu [b], Zhu-Quan Li [b], Jian-Hua Wei [b], Meng Wang [b], Xiao-Li Xie [b], Hong Liang [a,b,**]

[a] School of Chemistry of Nankai University, Tianjin 300071, PR China
[b] Guangxi Key Laboratory for the Chemistry and Molecular Engineering of Medicinal Resources, School of Chemistry & Chemical Engineering of Guangxi Normal University, Yucai Road 15, Guilin 541004, Guangxi, PR China

ARTICLE INFO

Article history:
Received 2 January 2013
Received in revised form
6 April 2013
Accepted 9 April 2013
Available online 17 April 2013

Keywords:
Aminophosphonate ester
Platinum(II) complexes
Synthesis
Crystal structure
Cytotoxicity
Action mechanism

ABSTRACT

New platinum(II) complexes containing aminophosphonate ester were synthesized and fully characterized, which were found to possess better solubility in both organic solvents and water than cisplatin. These platinum(II) complexes exhibited considerable cytotoxicity against tumor cells MG-63, SK-OV-3, HepG2, BEL-7404 and low cytotoxicity to normal human liver cells HL-7702. Their antitumor activities were achieved through the induction of cell apoptosis and the cell cycle arrest at G1 phase. The electrophoretic mobility studies and CD spectral analysis revealed that the binding mode of complex **6** to DNA might be different from that of cisplatin.

1. Introduction

Despite cisplatin (cis-diamminedichloroplatinum(II), CDDP)-based chemotherapy is curative for testicular germ cell tumors (TGCT) and constitutes a component of standard treatment regimes for ovarian, cervical, bladder, head and neck, small cell and non-small-cell lung cancers, the development of platinum drugs with improved antitumor activity continues to be a productive field of research [1,2]. Currently, the main focus concentrates on designing cytotoxic agents possessing either oral bioavailability, fewer side effects, or being able to circumvent intrinsic or acquired CDDP resistance, which is a major clinical problem [3,4]. To achieve these goals, chemists employed different strategies for the development of new platinum anticancer agents with different action mechanisms and broader ranges of antitumor activity [5,6]. Especially, in the past two decades, new functional ligands have been used to coordinate platinum and targeted drugs have been designed as an important strategy to overcome the side effects of cisplatin [7,8].

Because alkaline phosphatase is known to be overexpressed in the extracellular space of specific tumor cells such as ovarian and hepatic carcinoma cells [9,10] and the phosphate groups also exhibit high affinity to calcium ions, introduction of a phosphate group has been used to design targeted cisplatin analogs [11,12]. Since phosphonate esters can be hydrolyzed under biological conditions, phosphonate esters were used as a strategy to increase solubility and enhance transport through cellular membrane [11,12]. Platinum complexes incorporating functional phosphoric moieties for targeting cancer cells were first reported by Keppler and co-workers in the early 1990s [13]. More recently, Natile, Bose and Guo also reported platinum phosphonate complexes and found that some of them had a cytotoxic mechanism different from that of cisplatin [7,8,14,15]. However, except for Guo's work, most of published researches attached phosphonate groups to the platinum center as leaving groups. When the functional moieties are attached to platinum as leaving groups, they may detach during the complicated physiological process even before reaching the targeted tissues. As a result, the functional groups of the complexes will be lost. Therefore, one of the key factors for cancer targeting is to use non-leaving functional moieties to guide the platinum to specific tissues.

* Corresponding author. Tel./fax: +86 773 2120958.
** Corresponding author. School of Chemistry of Nankai University, Tianjin 300071, PR China.
E-mail addresses: chenzfubc@yahoo.com, chenzfgxnu@yahoo.com (Z.-F. Chen), hliang@gxnu.edu.cn (H. Liang).

0223-5234/$ – see front matter © 2013 Elsevier Masson SAS. All rights reserved.
http://dx.doi.org/10.1016/j.ejmech.2013.04.024

Aminophosphonic acids are structural analogs of natural aminocarboxylic acid. The functionalized aminophosphonic acids, especially, α-aminoalkyl-phosphonic derivatives, are a class of important compounds that exhibit intriguing biological activities in the pharmacological and agrochemical fields [16–19]. We have designed and synthesized a series of platinum(II) complexes containing aminophosphonate ester groups recently [20]. As the continuation of this series of researches, herein, we reported six platinum complexes containing new functional ligands of α-aminoalkyl-phosphonate ester derivatives as non-leaving groups. The anticancer structure–property relationship was established for platinum(II) complexes with various alkyl chain lengths $(CH_2)_m$ and three electron-donating and lipophilic methoxy substituents (R1–R3), in which these amides are known to have the potential to induce cell apoptosis [21,22].

2. Results and discussion

2.1. Synthesis

The aminophosphonate ester derivatives (**L^a**–**L^f**) were prepared from pyridinealdehyde, diethylphosphite and various amines via one-step synthetic route (Scheme 1). The products were characterized by elemental analysis, ^{1}H NMR, ^{13}C NMR and ESI-MS spectroscopy.

Corresponding *cis*-dichloroplatinum(II) complexes **1**–**6** were obtained by reacting *cis*-Pt(DMSO)$_2$Cl$_2$ with **L^a**–**L^f** in anhydrous dichloromethane and ethanol (1:1), respectively (Scheme 2).

The synthesized platinum(II) complexes were characterized by elemental analysis, ^{1}H NMR, ^{13}C NMR and ESI-MS spectroscopy as well as single crystal X-ray diffraction analysis (for complexes **1**, **3**, **5**, **6**).

2.2. Structures of platinum(II) complexes

The crystal structures of complexes **1**, **3**, **5** and **6** indicated that the platinum centers adopt an approximately square-planar geometry in which the dihedral angle between the pyridyl ring and Pt(II) coordination plane is 13.2° (complex **1**), 9.2° (complex **3**), 14.7° (complex **5**) and 7.1° (complex **6**). Selected bond lengths and angles are given in the captions of Figs. 1 and 2, which are within the normal range expected for Pt(II) complexes. One notable feature is that the carbon atom attached to P forms a half chair conformation with respect to the platinum coordination plane in all complexes, which is consistent with the steric interaction between the phosphonate ester moiety and the platinum coordination plane. The major structural distinctions among the complexes are the presence or absence of the three electron-donating and lipophilic methoxy groups at the C_3, C_4 and C_5 of the benzene ring, and the different spatial separations of the benzene ring from the platinum coordination plane. Additionally, complexes **1**–**6** exhibited higher solubility in both organic solvents and water compared with cisplatin.

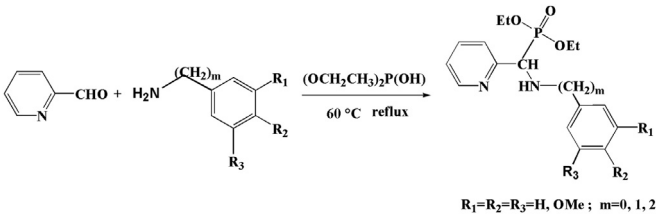

Scheme 1. Synthesis route of aminophosphonate esters.

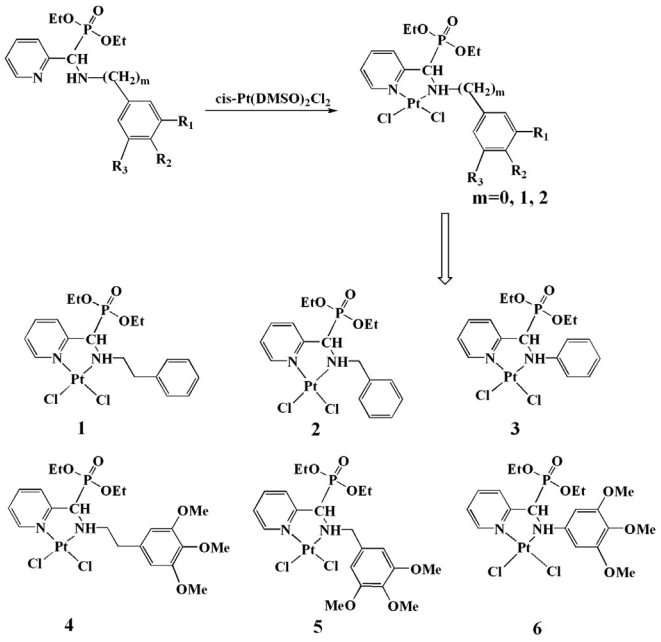

Scheme 2. Synthesis route of the platinum(II) complexes.

2.3. In vitro cytotoxic activity

The *in vitro* cytotoxicities of complexes **1**–**6** against MG-63, SK-OV-3, HepG2, BEL-7404 and HL-7702 cell lines were investigated by MTT method and compared with those of cisplatin. As shown in Table 1, the IC_{50} values of complexes **1**–**6** against tumor cell lines MG-63, SK-OV-3, HepG2 were higher than that of cisplatin. However, they exhibited lower IC_{50} (higher cytotoxicity) toward BEL-7404 than cisplatin. Complex **6** showed the highest cytotoxicity against BEL-7404 cell line. In addition, complexes **1**–**6** displayed lower cytotoxicities to normal human liver cells HL-7702 than to the tested tumor cells, and there was about an order of magnitude of difference. Comparison of the cytotoxicity of complexes **1** and **4**, **2** and **5**, **3** and **6** against the BEL-7404 tumor cells indicated that the presence of three methoxy groups at the C_3, C_4 and C_5 of the benzene ring enhanced cytotoxicity. Similar trends were observed for complexes **1** and **4**, **2** and **5**, **3** and **6** toward the other four tested tumor cell lines. Therefore, structures with the shortest distance of the phenyl ring to the platinum complex and the presence of the methoxy groups at the C_3, C_4 and C_5 of the benzene ring exhibited the highest cytotoxicity.

2.4. Apoptosis study by flow cytometry

Apoptosis is the programmed cell death that controls the development and homeostasis of multicellular organisms by elimination of aged, damaged, or mutated cells, which has been shown to be the key cellular event responsible for the anticancer activity of most of the anticancer drugs [23]. To determine whether the observed cell death induced by the complexes was due to apoptosis, the interaction of BEL-7404 cells with complex **6** was further investigated using an Annexin V-FITC/propidium iodide assay (Fig. 3). As phosphatidylserine (PS) exposure usually precedes loss of plasma membrane integrity in apoptosis, the presence of annexin V+/PI− cells is considered as an indicator of apoptosis. When treated with complex **6**, the population of annexin V+/PI− cells (Q4) was 50.8%, which suggested that apoptotic death was induced in BEL-7404 cells.

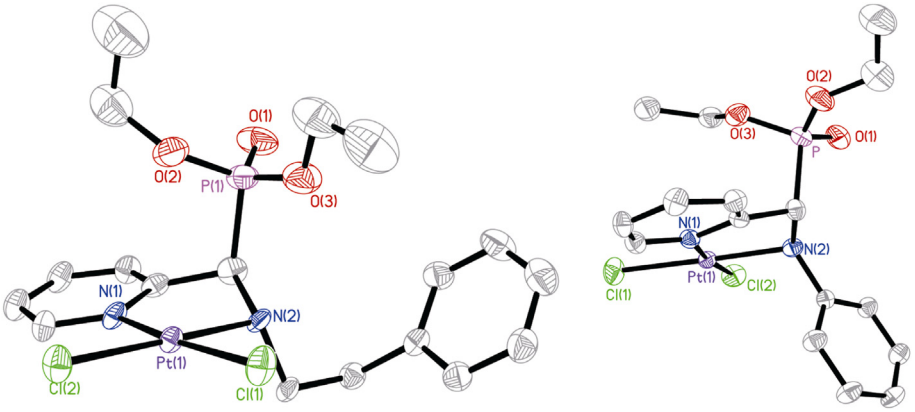

Fig. 1. ORTEP drawings of **1** (left) and **3** (right). The hydrogen atoms have been omitted for clarity. Selected bond lengths (Å) and angles (°) for **1**: Pt(1)–N(1) 2.0191(71), Pt(1)–N(2) 2.0555(74), Pt(1)–Cl(2) 2.3089(24), Pt(1)–Cl(1) 2.2830(21); N(1)–Pt(1)–N(2) 171.53(24), N(1)–Pt(1)–Cl(2) 95.69(23), N(1)–Pt(1)–Cl(1) 171.53(24), N(2)–Pt(1)–Cl(2) 177.66(21), N(2)–Pt(1)–Cl(1) 89.55(21), Cl(2)–Pt(1)–Cl(1) 92.75(9); for **3**: Pt(1)–N(1) 2.0069(84), Pt(1)–N(2) 2.0699 (102), Pt(1)–Cl(2) 2.2857 (30), Pt(1)–Cl(1) 2.2953 (33); N(1)–Pt(1)–N(2) 83.48(34), N(1)–Pt(1)–Cl(2) 173.43 (29), N(1)–Pt(1)–Cl(1) 94.10 (27), N(2)–Pt(1)–Cl(2) 90.55 (25), N(2)–Pt(1)–Cl(1) 177.54 (22), Cl(2)–Pt(1)–Cl(1) 91.84 (12).

2.5. Mitochondrial membrane potential detection

Mitochondria act as a point of integration for apoptotic signals originating from both the extrinsic and intrinsic apoptotic pathways. Mitochondrial dysfunction and the release of apoptogenic factors are critical events in triggering various apoptotic pathways [24,25]. Loss of mitochondrial membrane potential is an important indicator of mitochondrial dysfunction. To delineate the importance of mitochondria in complex **6** induced apoptosis, the changes of mitochondrial membrane potential were measured by the JC-1 probe, which was dispersed from aggregated form (red fluorescence) to the monomeric form (green fluorescence) when mitochondrial membrane potential was lost. As shown in Fig. 4, cells treated with complex **6** exhibited a significant decrease in mitochondria membrane potential as indicated by a notable shift in the ratio of green/red fluorescence versus control. These results suggested that mitochondria were involved in the initiation of apoptosis.

2.6. Caspase-3 activation assay

The Caspase family is well characterized as playing a crucial role in modulation of programmed cell death (PCD), which is a genetically regulated, evolutionarily conserved process with numerous links to many human diseases, most notably cancer [26]. Caspase-3 is able to directly degrade multiple substrates including structural and regulatory proteins. Thus, therapeutic strategies designed to stimulate apoptosis by activating Caspase-3 may help in combating cancer caused by apoptosis deficiency. Some small molecules have been developed to be selective activators of Caspase-3. We have therefore investigated whether the Caspase-3 was activated when BEL-7404 cells were exposed to complex **6**. As shown in Fig. 5, cells treated with complex **6** had a significant increase in the activity of caspase-3 as indicated by a notable shift in the ratio of green/dark fluorescence versus control.

2.7. Cell cycle analysis

The cell cycle is a set of events that result in cell growth and division into two daughter cells. The cell cycle is divided into G1, S, G2, and M stages. To determine whether the suppression of cancer cell growth by the platinum complexes was caused by cell cycle arrest, the BEL-7404 cells were treated with complex **6** and cisplatin respectively at their IC_{50} concentrations and the cell cycle phases were assayed via assessing the DNA content of cells stained with

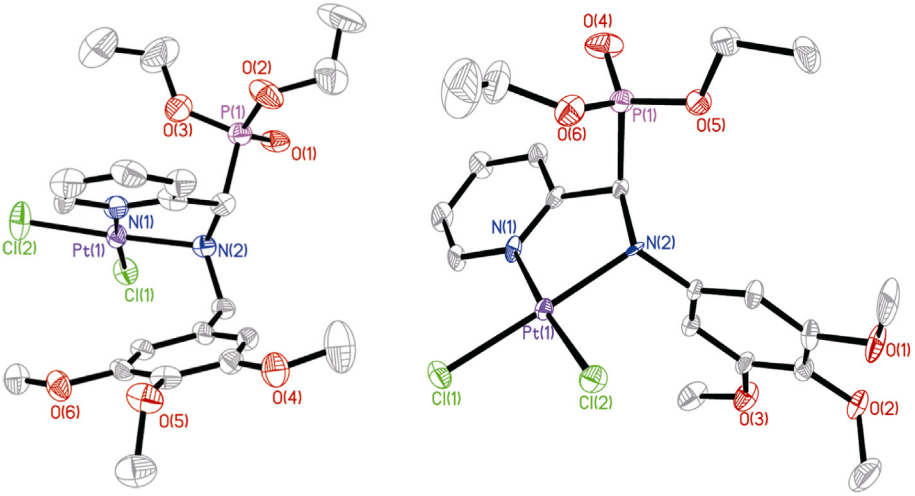

Fig. 2. ORTEP drawing of complexes **5** (left) and **6** (right), and the hydrogen atoms have been omitted for clarity. Selected bond lengths (Å)angles (°), for **5**: Pt(1)–N(1) 1.9965 (118), Pt(1)–N(2) 2.0560(90), Pt(1)–Cl(1) 2.3045(35), Pt(1)–Cl(2) 2.2928(32), N(1)–Pt(2)–N(2) 81.93(38), Cl(1)–Pt(2)–N(1) 173.60(30), Cl(2)–Pt(2)–N(1), 95.19 (30), N(2)–Pt(2)–Cl(1) 92.21(27), N(2)–Pt(2)–Cl(2) 176.71(28), Cl(1)–Pt(2)–Cl(2) 90.75(14); for **6**: Pt(1)–N(1) 2.0045(82), Pt(1)–N(2) 2.0571(68), Pt(1)–Cl(1) 2.2908(23), Pt(1)–Cl(2) 2.2866(26), N(1)–Pt(1)–N(2) 83.65(32), N(1)–Pt(1)–Cl(1) 94.77(22), N(1)–Pt(1)–Cl(2) 174.70(21), Cl(1)–Pt(1)–N(2) 178.31(22), Cl(2)–Pt(1)–N(2) 91.07(25), Cl(2)–Pt(1)–Cl(2) 90.51(10).

Table 1
IC_{50} (μM) values for complexes **1**–**6** against four human tumor cells and normal human liver cells.

Complex	MG-63	SK-OV-3	HepG2	BEL-7404	HL-7702
1	21.2	45.3	25.5	26.5	123.7
2	18.3	22.5	>50	32.1	148.5
3	>50	48.2	42.5	24.8	158.1
4	22.3	32.5	36.2	21.2	98.5
5	25.2	>50	18.2	17.6	114.9
6	21.4	18.2	25.2	12.5	105.4
Cisplatin[a]	9.5	6.4	11.5	132.8	86.0

[a] Cisplatin was used as positive control.

propidium iodide as measured by flow cytometry. The flow cytometric data for the BEL-7404 cells treated with complex **6** and cisplatin are shown in Fig. 6. Treatment of cells with complex **6** for 24 h enhanced cell-cycle arrest at the G1 phase, resulting in population increase in the G1 phase (70.65%) compared with the control cells (35.36%), and the populations of the S and G2 phase decreased only to a certain extent compared with the control cells. We speculated that the decrease of populations in S and G2 phases was the direct result of the population increase in G1 phase. However, cisplatin resulted in population increase in the S phase (48.11% and 35.36% for cisplatin and control, respectively), which is in agreement with the literature studies regarding cell cycle arrest by cisplatin [27]. Therefore, the mechanism of the suppression of tumor cells' growth by the title platinum(II) complexes might be different from that of cisplatin.

2.8. Interaction with pUC19 plasmid DNA

Since these platinum complexes possess the classic *cis*-dichloro coordination mode similar to cisplatin, we compared their interactions with ct-DNA with that of cisplatin. As shown by the gel electrophoresis experiments (Fig. 7), complex **6** induced a small change in the migration rate of the negatively supercoiled band of pUC19 plasmid DNA at 20 μM, and steadily decreased the DNA migration rate with the increase of concentrations. The migration rate of Form I DNA abruptly decreased when the concentration of complex **6** reached 60 μM, but it then increased notably when the concentration of complex **6** was further increased to 70 μM. In contrast, cisplatin induced no change in migration rate at concentrations below 40 μM and steadily decreased the DNA migration rate at concentrations greater than 40 μM. These results suggested that our platinum complexes might interact with DNA via different mechanism from cisplatin.

2.9. Circular dichroism spectral analysis

Circular dichroism (CD) is a useful technique to assess whether nucleic acids undergo conformational changes as a result of complex

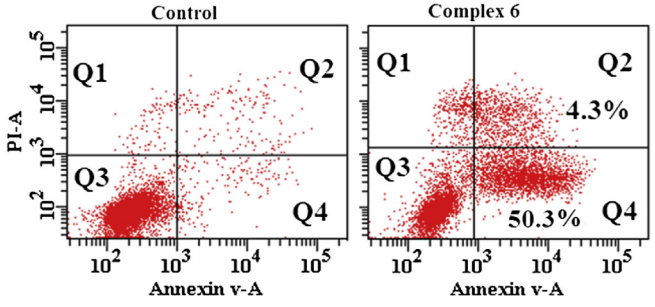

Fig. 3. Annexin V/propidium iodide assay of BEL-7404 cells treated by complex **6** (at IC_{50} concentration) measured by flow cytometry.

formation or changes in environment [28,29]. The normal ct-DNA has a right-handed chiral conformation and exists in B-form in solution. The CD spectrum of DNA is very sensitive to its conformational changes. It is generally accepted that covalent binding and intercalative binding can influence the tertiary structure of DNA and induce changes in the CD spectra of DNA, whereas other non-covalent binding modes such as electrostatic interaction or groove binding does not significantly perturb the CD spectra [30].

The CD spectrum of ct-DNA shows a positive absorbance peak at *ca.* 270 nm and a negative absorbance peak at *ca.* 245 nm, due to the π–π base stacking of DNA and the right-hand helicity of B-form DNA, respectively [31]. As shown in Fig. S1 (see ESI), the addition of complex **6** at the concentration of 5×10^{-6} M to 2×10^{-4} M did not perturb the positive absorbance of DNA obviously while the negative absorbance of DNA decreased. The changes in the CD spectra of the DNA upon addition of cisplatin were different from that induced by the addition of complex **6**, which strongly suggested that complex **6** has different binding mode toward ct-DNA. The CD result is in agreement with the pUC19 plasmid DNA assay.

3. Conclusions

Six new mononuclear platinum complexes **1**–**6** containing aminophosphonate esters as the non-leaving group were synthesized and fully characterized. Cytotoxicity assay of complexes **1**–**6** against MG-63, SK-OV-3, HepG2, BEL-7404 and HL-7702 cells showed that complex **6** exhibited the highest cytotoxicity against BEL-7404 cell line, which could be attributed to the structural features including the shortest separation phenyl ring from the platinum complex and the presence of methoxy groups at the C_3, C_4 and C_5 of the benzene ring. Complex **6** induced apoptosis in tumor cells and G1 cell cycle arrest, which is different from cisplatin that induces S phase cell cycle arrest. The electrophoretic mobility studies and CD spectral analysis revealed that the binding mode of complex **6** to DNA might be different from that of cisplatin. Further studies of this type of new platinum complexes could yield new leads to improve the potency and selectivity of platinum anticancer drugs.

4. Experimental

4.1. Materials and reagents

All chemicals, unless otherwise noted, were purchased from Sigma and Alfa Aesar. All materials were used as received without further purification unless noted specifically. Tris–HCl–NaCl (TBS) buffer solution (5 mM Tris, 50 mM NaCl, pH adjusted to 7.35 by titration with hydrochloric acid using a Sartorius PB-10 pH meter, Tris = tri(hydroxymethyl)aminomethane) was prepared using double distilled water. The TBE buffer (1×) and DNA loading buffer (6×) were commercially available. Calf thymus DNA (ct-DNA) was purchased from Sino-American Biotech Co., Ltd. (Beijing). Ct-DNA gave a UV absorbance ratio at 260–280 nm of ~1.85:1, indicating that the DNA was effectively free of protein. The DNA concentration per nucleotide was determined spectrophotometrically by employing a molar absorption coefficient (6600 M^{-1} cm^{-1}) at 260 nm. The stock solution of pUC19 plasmid DNA (250 μg/mL) was purchased from Takara Biotech Co., Ltd.

4.2. Instrumentation

^1H NMR, ^{13}C NMR spectra were recorded on a Bruker AV-500 NMR spectrometer with $CDCl_3$ or DMSO-d_6 as solvent. Elemental analyses (C, H, and N) were carried out on a PerkinElmer Series II CHNS/O 2400 elemental analyzer. ESI-MS spectra for the

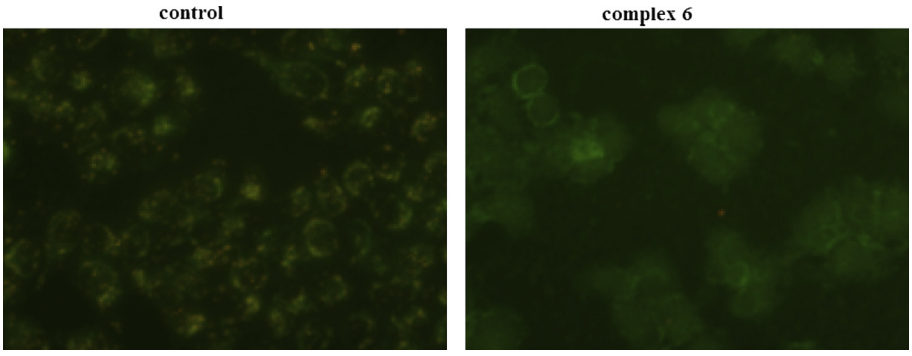

Fig. 4. Loss of $\Delta\Psi m$ induced by complex **6**. Cells were treated with complex **6** for 3 h and examined by JC-1 under fluorescent microscope.

characterization of complexes **1**–**6** were performed on Thermofisher Scientific Exactive LC-MS Spectrometer.

4.3. Synthesis

4.3.1. Synthesis of the ligands

General procedure for the synthesis of aminophosphonate esters ligands [29]. Equimolar amounts (0.2 mol) of pyridinealdehyde, diethylphosphite and phenyl-amines were refluxed for 1 h at 60 °C. After the reaction mixture was cooled to room temperature, the oily residue was purified on a silica gel column (petroleum ether:ethyl acetate = 1:1). Yellow oil-like product was obtained.

*4.3.1.1. Diethyl(phenethylamino)(2-pyridinyl)methylphosphonate (**L**^{a}).* ^{1}H NMR (500 MHz, $CDCl_3$) δ 8.54 (dd, J = 4.8, 1.2 Hz, 1H), 7.62 (td, J = 7.7, 1.7 Hz, 1H), 7.37 (dd, J = 8.1, 1.3 Hz, 1H), 7.22 (t, J = 7.4 Hz, 2H), 7.19–7.11 (m, 4H), 4.21 (d, J = 21.3 Hz, 1H), 4.10–4.03 (m, 2H), 4.02–3.95 (m, 1H), 3.89 (tdd, J = 10.3, 7.7, 5.2 Hz, 1H), 2.81–2.72 (m, 4H), 1.23 (t, J = 7.1 Hz, 3H), 1.14 (t, J = 7.1 Hz, 3H). ^{13}C NMR (125 MHz, $CDCl_3$) δ 156.39 (s), 149.19 (s), 139.82 (s), 136.41 (s), 128.74 (d, J = 9.9 Hz), 128.32 (s), 126.08 (s), 123.42 (d, J = 4.7 Hz), 122.62 (d, J = 2.5 Hz), 63.35–63.06 (m), 62.79 (d, J = 7.0 Hz), 61.95 (d, J = 26.9 Hz), 49.98 (d, J = 16.4 Hz), 36.32 (s), 16.37 (d, J = 5.7 Hz), 16.26 (d, J = 5.7 Hz). ESI-MS: m/z 349.17 [**L**^{a} + H]$^{+}$.

*4.3.1.2. Diethyl(benzylamino)(2-pyridinyl)methylphosphonate (**L**^{b}).* ^{1}H NMR (500 MHz, $CDCl_3$) δ 8.60 (dd, J = 4.8, 1.1 Hz, 1H), 7.66 (td, J = 7.7, 1.4 Hz, 1H), 7.42 (dd, J = 7.9, 1.0 Hz, 1H), 7.30–7.26 (m, 4H), 7.25–7.18 (m, 2H), 4.20 (d, J = 21.8 Hz, 1H), 4.17–4.09 (m, 2H), 4.09–4.02 (m, 1H), 3.96–3.87 (m, 1H), 3.81 (d, J = 13.3 Hz, 1H), 3.59 (d, J = 13.3 Hz, 1H), 1.27 (t, J = 7.1 Hz, 3H), 1.17 (t, J = 7.1 Hz, 3H). ^{13}C NMR (125 MHz, $CDCl_3$) δ 156.18 (s), 149.32 (s), 139.30 (s), 136.39 (s), 128.40 (s), 128.33 (s), 127.11 (s), 123.82 (d, J = 4.8 Hz), 122.65 (d, J = 2.5 Hz), 63.19 (d, J = 6.8 Hz), 62.76 (d, J = 6.9 Hz), 52.10 (s), 51.97 (s), 16.42 (d, J = 5.8 Hz), 16.27 (d, J = 5.8 Hz). ESI-MS: m/z 335.13 [**L**^{b} + H]$^{+}$.

*4.3.1.3. Diethyl anilino(2-pyridinyl)methylphosphonate (**L**^{c}).* ^{1}H NMR (500 MHz, $CDCl_3$) δ 8.69 (d, J = 4.6 Hz, 1H), 7.81 (t, J = 7.7 Hz, 1H), 7.63 (d, J = 8.0 Hz, 1H), 7.40–7.35 (m, 1H), 7.05 (dd, J = 11.2, 4.4 Hz, 2H), 6.68–6.59 (m, 3H), 4.02–3.99 (m, 4H), 3.93–3.86 (m, 1H), 1.22 (d, J = 7.0 Hz, 3H), 1.11 (t, J = 7.0 Hz, 3H). ^{13}C NMR (125 MHz, $CDCl_3$) δ 154.96 (s), 146.88 (s), 145.83 (d, J = 12.7 Hz), 139.56 (s), 129.23 (s), 128.03 (s), 123.59 (d, J = 80.4 Hz), 118.86 (s), 113.87–113.27 (m), 61.82 (s), 61.77 (s), 56.80 (s), 16.27 (s), 16.22 (s). ESI-MS: m/z 321.14 [**L**^{c} + H]$^{+}$

*4.3.1.4. Diethyl 2-pyridinyl[(3,4,5-trimethoxyphenethyl)amino]methylphosphonate (**L**^{d}).* ^{1}H NMR (500 M Hz, $CDCl_3$) δ 8.59 (s, 1H), 7.67 (d, J = 7.7, 1.6 Hz, 1H), 7.46 (d, J = 7.0 Hz, 1H), 7.28 (m, 1H), 6.44 (d, J = 5.9 Hz, 2H), 4.21 (dd, J = 11.9, 5.0 Hz, 2H), 4.14–4.05 (m, 2H), 3.84 (d, J = 9.0 Hz, 1H), 3.68–3.54 (m, 9H), 3.15 (s, 2H), 3.01 (s, 2H), 1.26 (m, 3H), 1.13 (m, 3H). ^{13}C NMR (125 MHz, $CDCl_3$) δ 157.04 (s), 152.13 (s), 149.34 (s), 137.12 (s), 136.48 (s), 134.47 (s), 123.81 (d, J = 4.1 Hz), 121.72 (s), 105.14 (s), 62.89 (d, J = 7.8 Hz), 62.87 (d, J = 6.0 Hz), 61.41 (s), 60.17 (s), 60.03 (s), 55.42 (s), 37.21 (s) 16.31 (d, J = 4.5 Hz), 16.17 (d, J = 4.3 Hz) ESI-MS: m/z 439.18 [**L**^{d} + H]$^{+}$.

*4.3.1.5. Diethyl 2-pyridinyl[(3,4,5-trimethoxybenzyl)amino]methylphosphonate (**L**^{e}).* ^{1}H NMR (500 M Hz, $CDCl_3$) δ 8.56 (s, 1H), 7.63 (d, J = 7.1 Hz, 1H), 7.36 (d, J = 6.3 Hz, 1H), 7.21–7.12 (m, 1H), 6.46 (d, J = 5.2 Hz, 2H), 4.17 (dd, J = 21.9, 6.0 Hz, 1H), 4.12–4.03 (m, 2H), 4.02–3.95 (m, 1H), 3.89 (dd, J = 9.3, 5.7 Hz, 1H), 3.79–3.71 (m, 10H), 3.51 (d, J = 12.8 Hz, 1H), 1.26–1.21 (m, 3H), 1.13 (q, J = 7.2 Hz, 3H). ^{13}C NMR (125 MHz, $CDCl_3$) δ 156.08 (s), 153.12 (s), 149.26 (s), 136.88 (s), 136.36 (s), 134.97 (s), 123.87 (d, J = 4.7 Hz), 122.68 (d, J = 2.3 Hz), 105.14 (s), 63.09 (d, J = 6.8 Hz), 62.77 (d, J = 7.0 Hz), 61.49 (s), 60.77 (s), 60.27 (s), 55.99 (s), 16.42 (d, J = 5.7 Hz), 16.26 (d, J = 5.6 Hz). ESI-MS: m/z 425.19 [**L**^{e} + H]$^{+}$.

*4.3.1.6. Diethyl 2-pyridinyl(3,4,5-trimethoxyanilino)methylphosphonate (**L**^{f}).* ^{1}H NMR (500 MHz, $CDCl_3$) δ 8.56 (s, 1H), 7.63 (d, J = 5.6 Hz, 1H), 7.49 (d, J = 7.4 Hz, 1H), 7.18 (s, 1H), 5.21 (d, J = 41.8 Hz, 1H), 4.92 (d,

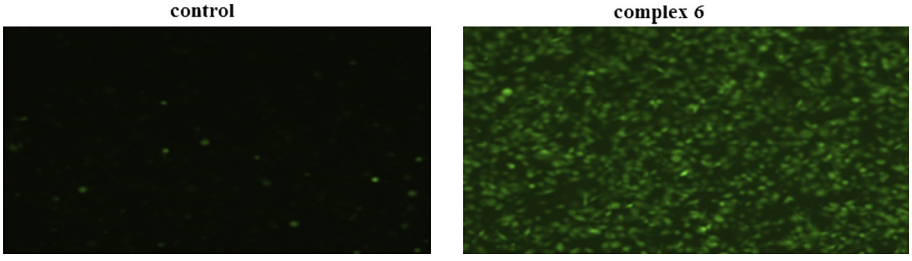

Fig. 5. Activation of Caspase-3 induced by complex **6**, examined by FITC-DEVD-FMK under a fluorescent microscope.

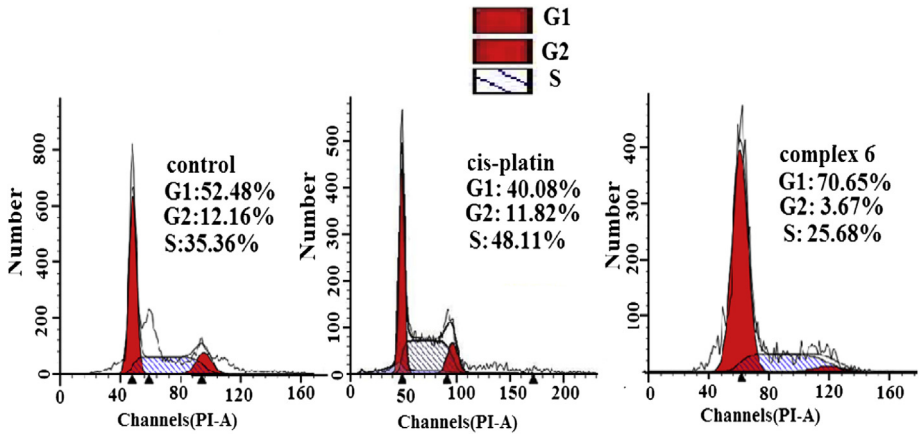

Fig. 6. Cell cycle analysis by flow cytometry of BEL-7404 cells treated with complex **6** and cisplatin at IC_{50} concentrations.

J = 22.1 Hz, 1H), 4.10 (dd, J = 19.5, 12.8 Hz, 2H), 4.00 (d, J = 2.8 Hz, 1H), 3.86 (s, 1H), 3.68 (dd, J = 11.6, 4.3 Hz, 9H), 1.26 (d, J = 6.2 Hz, 3H), 1.13 (d, J = 6.2 Hz, 3H). ^{13}C NMR (125 MHz, $CDCl_3$) δ 156.03 (s), 153.76 (s), 149.06 (s), 143.23 (d, J = 13.0 Hz), 136.83 (s), 130.67 (s), 128.82 (s), 122.81 (d, J = 4.4 Hz), 91.69 (s), 63.46 (d, J = 6.9 Hz), 63.26 (d, J = 7.1 Hz), 60.96 (s), 59.14 (s), 57.94 (s), 55.84 (s), 16.41 (d, J = 5.7 Hz), 16.22 (d, J = 5.7 Hz). ESI-MS: m/z 411.12[$\mathbf{L}^{\mathbf{f}}$ + H]$^+$.

4.3.2. Synthesis of the platinum complexes

General procedure for the synthesis of the platinum complexes: To a solution of *cis*-Pt(DMSO)$_2$Cl$_2$ (84 mg, 0.2 mmol) was added $\mathbf{L}^{\mathbf{a-f}}$ (0.2 mmol) dissolved in 30 mL mixtures of anhydrous dichloromethane and ethanol (1:1). The mixture was stirred in the dark at room temperature for 1 day. The resulting yellow solution was filtered and crystals or solid powders were obtained by slow evaporation of filtrate solution.

*4.3.2.1. Complex **1**.* ^{1}H NMR (500 MHz, DMSO-d_6) δ 9.05 (dd, J = 27.1, 5.8 Hz, 1H), 8.24 (t, J = 7.7 Hz, 1H), 7.66 (dd, J = 18.6, 7.2 Hz, 1H), 7.62–7.57 (m, 1H), 7.28 (d, J = 7.3 Hz, 2H), 7.23 (s, 2H), 7.21 (d, J = 5.4 Hz, 1H), 4.34–4.10 (m, 4H), 3.98–3.85 (m, 1H), 3.10 (d, J = 10.5 Hz, 2H), 3.03 (d, J = 8.2 Hz, 2H), 1.32–1.26 (m, 3H), 1.21 (t, J = 6.9 Hz, 3H). ^{13}C NMR (125 MHz, DMSO-d_6) δ 160.70 (d, J = 8.4 Hz), 148.49 (s), 139.76 (s), 137.98 (s), 129.20 (s), 128.98 (s), 127.00 (s), 125.72 (s), 124.72 (s), 65.30 (d, J = 6.5 Hz), 64.14 (d, J = 6.5 Hz), 58.66 (d, J = 10.7 Hz), 48.81 (s), 34.14 (s), 16.55 (s), 16.50 (s). ESI-MS: m/z 614.42 [M + H]$^+$. Elemental analysis calculated: C, 35.37; H, 4.02; N, 4.65; Found: C, 35.25; H, 3.94; N, 4.57.

*4.3.2.2. Complex **2**.* ^{1}H NMR (500 MHz, DMSO-d_6) δ 8.95 (dd, J = 21.3, 4.8 Hz, 1H), 8.02 (t, J = 7.4 Hz, 1H), 7.61 (d, J = 18.6 Hz, 1H), 7.40–7.38 (m, 1H), 7.13 (t, J = 6.7 Hz, 2H), 6.82 (t, J = 7.2 Hz, 2H), 6.66 (t, J = 5.7 Hz, 1H), 5.31 (d, J = 15.8 Hz, 1H), 4.42–4.31 (m, 4H), 3.53 (d, J = 11.5 Hz, 2H) 1.24 (t, J = 5.1 Hz, 3H), 1.12 (t, J = 7.0 Hz, 3H). ^{13}C NMR (125 MHz, DMSO-d_6) δ 158.14 (s), 151.42 (s), 141.33 (s), 137.42 (s), 129.11 (s), 128.73 (s), 127.71 (s), 122.82 (s), 121.63 (s), 63.19 (d, J = 5.6 Hz), 62.86 (d, J = 7.3 Hz), 53.14 (s), 50.87 (s), 16.32 (d, J = 4.8 Hz), 16.17 (d, J = 5.1 Hz). ESI-MS: m/z 599.12 [M + H]$^+$. Elemental analysis calculated: C, 34.14; H, 3.74; N, 4.58; Found: C, 34.07; H, 3.70; N, 4.67.

*4.3.2.3. Complex **3**.* ^{1}H NMR (500 MHz, DMSO-d_6) δ 8.55 (d, J = 4.7 Hz, 1H), 7.80 (t, J = 7.7 Hz, 1H), 7.60 (d, J = 7.9 Hz, 1H), 7.33–7.28 (m, 1H), 7.03 (t, J = 7.7 Hz, 2H), 6.77 (d, J = 8.2 Hz, 2H), 6.56 (t, J = 7.2 Hz, 1H), 5.11 (d, J = 23.8 Hz, 1H), 4.11–4.03 (m, 2H), 3.95 (ddd, J = 17.3, 10.8, 5.1 Hz, 1H), 3.81 (tt, J = 14.9, 7.2 Hz, 1H), 1.20 (t, J = 7.1 Hz, 3H), 1.07 (t, J = 7.0 Hz, 3H). ^{13}C NMR (125 MHz, DMSO-d_6) δ 156.96 (s), 149.05 (s), 147.55 (d, J = 13.6 Hz), 137.30 (s), 129.87 (s), 129.11 (d, J = 30.3 Hz), 123.46 (d, J = 3.8 Hz), 123.32 (s), 117.71 (s), 114.00 (s), 63.09 (d, J = 6.8 Hz), 62.86 (d, J = 7.0 Hz), 56.89 (d, J = 150.1 Hz), 16.74 (d, J = 5.3 Hz), 16.52 (d, J = 5.5 Hz). ESI-MS: m/z 585.13. Elemental analysis calculated: C, 32.89; H, 3.56; N, 4.68; Found: C, 32.83; H, 3.44; N, 4.79.

*4.3.2.4. Complex **4**.* ^{1}H NMR (500 MHz, DMSO-d_6) δ 9.01 (d, J = 4.8 Hz, 1H), 8.21 (t, J = 3.7 Hz, 1H), 7.41 (d, J = 7.9 Hz, 1H), 7.41 (t, J = 5.4 Hz, 1H), 6.72 (s, 2H), 4.29–4.22 (m, 2H), 4.12–4.10 (m, 4H), 4.08 (d, J = 12.5 Hz, 1H), 3.74 (s, 2H), 3.52–3.48 (s, 9H), 1.28 (t, J = 6.7 Hz, 3H), 1.16 (t, J = 7.4 Hz, 3H). ^{13}C NMR (125 MHz, DMSO-d_6) δ 160.61 (s), 150.41 (s), 150.51 (s), 148.32 (s), 142.14 (s), 137.80 (s), 128.43 (s), 124.65 (s), 124.16 (s), 111.04 (s), 109.49 (s), 65.24 (d, J = 4.5 Hz), 63.24 (d, J = 7.3 Hz), 60.42 (d, J = 11.4 Hz), 60.17 (s), 55.66 (d, J = 4.7 Hz), 55.33 (s), 41.26 (s), 16.30–16.28 (m), 16.43 (d, J = 3.9 Hz). ESI-MS: m/z 703.45 [M + H]$^+$. Elemental analysis calculated: C, 35.64; H, 4.24; N, 4.02; Found: C, 35.86; H, 4.30; N, 3.98.

*4.3.2.5. Complex **5**.* ^{1}H NMR (500 MHz, DMSO-d_6) δ 8.78 (d, J = 5.8 Hz, 1H), 8.01 (t, J = 7.7 Hz, 1H), 7.43 (d, J = 7.7 Hz, 1H), 7.33 (t, J = 6.4 Hz, 1H), 7.27 (s, 2H), 4.57–4.51 (m, 1H), 4.29–4.22 (m, 2H), 4.18–4.10 (m, 4H), 4.02 (d, J = 12.0 Hz, 1H), 3.78 (s, 3H), 3.77 (s, 6H), 1.25 (t, J = 7.0 Hz, 3H), 1.19 (t, J = 7.0 Hz, 3H). ^{13}C NMR (125 MHz,

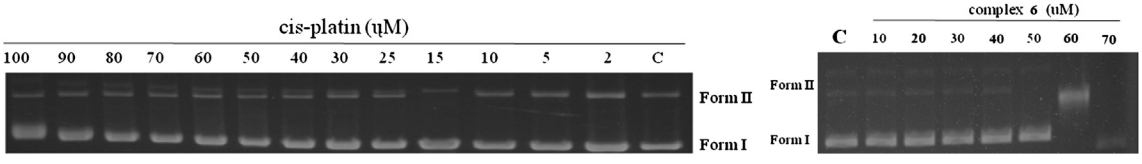

Fig. 7. Electrophoresis in agarose gel of pUC19 plasmid DNA (0.02 mg/mL, 30 μM base pair) incubated for 4 h at 37 °C with cisplatin, complex **6**, respectively. "C" represents control; the concentration of each platinum complex is indicated in the figure.

DMSO-d_6) δ 161.64 (d, J = 8.7 Hz), 152.80 (s), 152.54 (s), 147.55 (s), 142.04 (s), 138.80 (s), 128.83 (s), 125.65 (s), 124.79 (s), 110.01 (s), 109.91 (s), 65.27 (d, J = 6.5 Hz), 64.20 (d, J = 6.9 Hz), 60.58 (d, J = 10.4 Hz), 60.14 (s), 56.31 (d, J = 4.7 Hz), 56.27 (s), 16.58–16.49 (m), 16.33 (d, J = 5.9 Hz). ESI-MS: m/z 689.22 $[M + H]^+$. Elemental analysis calculated: C, 35.12; H, 4.01; N, 3.98; Found: C, 34.84; H, 4.09; N, 4.06.

4.3.2.6. Complex ***6****.* ^{1}H NMR (500 MHz, DMSO-d_6) δ 8.56 (d, J = 4.7 Hz, 1H), 7.81 (t, J = 7.7 Hz, 1H), 7.62 (t, J = 13.0 Hz, 1H), 7.34–7.25 (m, 1H), 6.12 (s, 2H), 5.14 (d, J = 23.8 Hz, 1H), 4.08 (p, J = 7.3 Hz, 2H), 3.96 (dt, J = 21.9, 7.2 Hz, 1H), 3.84–3.76 (m, 1H), 3.63 (d, J = 7.0 Hz, 6H), 3.62 (d, J = 2.9 Hz, 1H), 3.48 (s, 3H), 3.18 (s, 1H), 1.22 (t, J = 7.0 Hz, 3H), 1.08 (t, J = 7.0 Hz, 3H). ^{13}C NMR (125 MHz, DMSO-d_6) δ 157.14 (s), 153.62 (s), 148.97 (s), 144.13 (d, J = 14.6 Hz), 137.34 (s), 129.83 (s), 123.59 (s), 123.32 (s), 92.05 (s), 63.06 (d, J = 6.6 Hz), 62.84 (d, J = 6.8 Hz), 60.52 (s), 56.58 (s), 55.98 (s), 16.77 (d, J = 5.2 Hz), 16.54 (d, J = 5.5 Hz). ESI-MS: m/z 675.26 $[M + H]^+$. Elemental analysis calculated: C, 33.82; H, 3.62; N, 3.93; Found: C, 33.79; H, 3.88; N, 4.15.

4.3.3. X-ray crystallographic analysis

Suitable crystals of complexes **1**, **3**, **5**, **6** were grown from dichloromethane and ethanol (1:1). The single crystals were mounted on glass fibers, and crystal data were collected on a Bruker Smart Apex II CCD or Rigaku Mercury CCD diffractometer equipped with graphite monochromated Mo Kα radiation (λ = 0.71073 Å) at room temperature. Absorption correction were applied by using the multiscan program SADABS [32]. The structures were solved with direct methods and refined using SHELX-97 programs [33]. The non-hydrogen atoms were located in successive difference Fourier synthesis. The final refinement was performed by full-matrix least-squares methods with anisotropic thermal parameters for non-hydrogen atoms on F^2. The hydrogen atoms were added theoretically and riding on the concerned atoms. The crystallographic data and refinement details of the structures are summarized Table 2.

4.4. Cell lines, culture conditions and cytotoxicity assay (MTT assay)

The cell lines MG-63, SKOV-3, HepG2, BEL-7404 and HL-7702 were obtained from the Shanghai Cell Bank in the Chinese Academy of Sciences. Cell lines were grown in the RPMI-1640 medium supplemented with 10% (v/v) fetal bovine serum, 2 mM glutamine, 100 U/mL penicillin, and 100 U/mL streptomycin at 37 °C, in a highly humidified atmosphere of 95% air/5% CO_2. The cytotoxicities of complexes **1**–**6** against MG-63, SKOV-3, HepG2, BEL-7404 and HL-7702 cell lines were examined by the microculture tetrazolium (MTT) assay [34]. The experiments were carried out using reported procedure [35]. The growth inhibitory rate of treated cells was calculated using the data from three replicate tests as $(OD_{control} - OD_{test})/OD_{control} \times 100\%$. The compounds were incubated with various cell lines for 48 h at five different concentrations of complexes **1**–**6** dissolved in fresh media; the range of concentrations used is dependent on the complex. The final IC_{50} values were calculated by the Bliss method (n = 5). All tests were independently repeated at least three times.

4.5. Apoptosis assays by flow cytometry

The ability of platinum complex **6** to induce apoptosis is evaluated in BEL-7404 cell line using Annexin V conjugated with FITC and propidium iodide (PI) counterstaining by flow cytometry. BEL-7404 cells of exponential growth were inoculated in 6-well plates and cultured for 12 h before the platinum compounds were added to give the indicated final concentrations. After 48-hour incubation, cells were harvested, washed twice in phosphate-buffered saline (PBS), and resuspended in 100 μL binding buffer (including 140 mmol/L NaCl, 2.5 mmol/L $CaCl_2$ and 10 mmol/L Hepes/NaOH, pH 7.4) at a concentration of 1×10^6 cells/mL. Then cells were incubated with 5 μL of Annexin V-FITC (in buffer including 10 mmol/L NaCl, 1% bovine serum albumin, 0.02% NaN_3 and 50 mmol/L Tris, pH 7.4) and 10 μL PI (20 μg/mL) for 15 min at room temperature in the dark. Cells were kept shielded from light before being analyzed by flow cytometry using a Becton–Dickinson FACSCalibur.

4.6. Mitochondrial membrane potential detection

Cells incubated with IC_{50} concentration of complex **6** for 12 h in poly-HEMA coated 6-wells were collected and resuspended in fresh medium. After the addition of 0.5 mL JC-1 working solution, the cells were incubated in a 5% CO_2 incubator for 20 min at 37 °C. The staining solution was removed by centrifugation and cells were washed with JC-1 staining buffer twice. Cells having low membrane potential were

Table 2
Crystal data and structure refinement details for complexes **1**, **3**, **5**, **6**.

Formula	$C_{18}H_{27}Cl_2N_2O_4PPt$	$C_{16}H_{21}Cl_2N_2O_3PPt$	$C_{20}H_{29}Cl_2N_2O_6PPt$	$C_{19}H_{27}Cl_2N_2O_6PPt$
fw	632.38	586.30	690.40	676.39
T/K	293(2)	293(2)	293(2)	293(2)
Crystal system	Monoclinic	Orthorhombic	Triclinic	Triclinic
Space group	*P*21/*c*	*Pbca*	*P*-1	*P*-1
a, Å	15.4044(5)	5.4808(8)	11.7643(4)	9.0916(4)
b, Å	8.2538(2)	14.8321(10)	15.8123(10)	11.3273(6)
c, Å	18.9162(6)	17.5122(8)	16.3386(8)	12.2329(4)
α, °	90.00	90.00	61.921(6)	104.389(4)
β, °	107.911(4)	90.00	72.916(3)	95.129(4),
γ, °	90.00	90.00	88.301(4)	101.415(4)
V, Å^3	2288.53(12)	4021.0(4)	2541.9(2)	1183.32(10)
Z	4	8	4	2
D_c, g cm^{-3}	1.835	1.937	1.804	1.893
μ, mm^{-1}	6.460	7.339	5.830	6.257
GOF on F^2	1.034	1.018	1.014	1.029
Reflns (collected/unique)	10,669/4683	38,217/4113	20,992/10,383	9838/4849
R_{int}	0.0797	0.3935	0.1033	0.0998
R_1[a] ($I > 2\sigma(I)$)	0.0593	0.1123	0.0912	0.0645
wR_2[b] (all data)	0.1647	0.2445	0.2741	0.1497

[a] $R_1 = \Sigma||F_o| - |F_c||/\Sigma|F_o|$.
[b] $wR_2 = [\sum w(F_o^2 - F_c^2)^2 / \sum w(F_o^2)^2]^{1/2}$.

taken pictures under fluorescent microscope with excitation and emission at 485 and 535 nm, respectively (45×, Nikon).

4.7. Determination of caspase-3 activity

The activation of caspase-3 was examined using a caspase-3 (DEVD-FMK) conjugated to FITC as the fluorescent in situ marker in living cells (catalog #QIA91, Merck). FITC-DEVD-FMK is cell permeable, nontoxic, and irreversibly binds to activated caspase-3 in apoptotic cells. After exposure of BEL-7404 cell lines to complex **6** for 8 h, the cultures were washed twice with HBSS containing 0.1% BSA and then incubated with FITC-DEVD-FMK (1 μL/mL in EBSS) for 1 h in a 37 °C incubator with 5% CO_2. The FITC label in apoptotic cells was examined immediately under fluorescent microscope with excitation and emission at 485 and 535 nm, respectively (25×, Nikon).

4.8. Cell cycle analysis

BEL-7404 cell lines were maintained in Dulbecco's modified Eagle's medium with 10% fetal calf serum in 5% CO_2 at 37 °C. Cells were harvested by trypsinization and rinsed with PBS. After centrifugation, the pellet (10^5–10^6 cells) was suspended in 1 mL of PBS and kept on ice for 5 min. The cell suspension was then fixed by the dropwise addition of 9 mL precooled (4 °C) 100% ethanol with violent shaking. Fixed samples were kept at 4 °C until use. For staining, cells were centrifuged, resuspended in PBS, digested with 150 mL of RNase A (250 μg/mL), and treated with 150 mL of propidium iodide (PI) (0.15 mM), then incubated for 30 min at 4 °C. PI-positive cells were counted with a FACScan Fluorescence-activated cell sorter (FACS). The population of cells in each cell cycle phase was determined using Cell Modi FIT software (Becton Dickinson).

4.9. Agarose gel electrophoresis assay [36]

In plasmid DNA unwinding experiments, all compounds were prepared as 2×10^{-3} M stock solutions of DMSO and diluted to 10 and 100 μM by 1× TBE buffer. Compounds of various concentrations were mixed with 0.5 μg DNA and made up to a total 25 μL by TBE buffer so that the same experiment can be repeated twice. All samples were incubated at 25 °C in dark for 4 h. Then 12 μL of each sample mixed with 2 μL DNA loading buffer was electrophoresed at 5 V/cm through 0.8% agarose gel immersed in 1× TBE buffer solution for 60 min. Finally, the gel was stained with EB (1.27 μM) in dark for 30 min, followed by visualized on a BIO-RAD imaging system with a UV–vis transilluminator.

4.10. CD absorption spectrometry assay

In the CD absorption spectrometry, the working solution of each sample was prepared by using 1×10^{-4} M DNA and titrating the complexes into the DNA solution stepwise with the [DNA]/[compound] ratio ranging from 10:0.5 to 10:5. The working solution was incubated for 10 min after each addition and then its CD spectrum was recorded at 100 nm/min scan rate. The CD signals of the TBS were subtracted as the background.

4.11. Statistics

The data processing included the Student's *t*-test with $P \leq 0.05$ taken as significance level, using SPSS 13.0.

Acknowledgments

This work was supported by the National Natural Science Foundation of China (No. 21271051), National Basic Research Program of China (2012CB723501), IRT1225, and Natural Science Foundation of Guangxi Province (Nos. 2012GXNSFDA053005, 2012GXNSFDA385001) as well as "BAGUI Scholar" program of Guangxi province of China.

Appendix A. Supplementary material

Supplementary material related to this article can be found at http://dx.doi.org/10.1016/j.ejmech.2013.04.024.

References

[1] W. Voigt, A. Dietrich, H.J. Schmoll, Pharm. Unserer Zeit 35 (2006) 134–143.
[2] A. Dietrich, T. Mueller, R. Paschke, B. Kalinowski, T. Behlendorf, F. Reipsch, A. Fruehauf, H.J. Schmoll, C. Kloft, W. Voigt, J. Med. Chem. 51 (2008) 5413–5422.
[3] D. Lebwohl, R. Canetta, Eur. J. Cancer 34 (1998) 1522–1534.
[4] J.J. Wilson, S.J. Lippard, J. Med. Chem. 55 (2012) 5326–5336.
[5] E. Gabano, M. Ravera, D. Osella, Curr. Med. Chem. 16 (2009) 4544–4580.
[6] F. Kratz, I.A. Muller, C. Ryppa, A. Warnecke, ChemMedChem 3 (2008) 20–53.
[7] Z.Q. Xue, M. Lin, J. Zhu, J. Zhang, Y.Z. Li, Z. Guo, Chem. Commun. 46 (2010) 1212–1214.
[8] S.V. Zutphen, J. Reedijk, Coord. Chem. Rev. 249 (2005) 2845–2853.
[9] L.C. Chou, M.T. Tsai, M.H. Hsu, S.H. Wang, T.D. Way, C.H. Huang, H.Y. Lin, K.D. Qian, Y.Z. Dong, K.H. Lee, L.J. Huang, S.C. Kuo, J. Med. Chem. 53 (2010) 8047–8058.
[10] E. Kotsikorou, E. Oldfield, J. Med. Chem. 46 (2003) 2932–2944.
[11] F. Orsini, G. Sello, M. Sisti, Curr. Med. Chem. 17 (2010) 264–289.
[12] S. Piccinonna, N. Margiotta, C. Pacifico, A. Lopalco, N. Denora, S. Fedi, M. Corsinic, G. Natile, Dalton Trans. 41 (2012) 9689–9699.
[13] M. Galanski, S. Slaby, M.A. Jakupec, B.K. Keppler, J. Med. Chem. 46 (2003) 4946–4951.
[14] R. Sasanelli, A. Boccarelli, D. Giordano, M. Laforgia, F. Arnesano, G. Natile, C. Cardellicchio, M.A. Capozzi, M. Coluccia, J. Med. Chem. 50 (2007) 3434–3441.
[15] R.N. Bose, L. Maurmann, R.J. Mishur, L. Yasui, S. Gupta, W.S. Grayburn, H. Hofstetter, T. Salley, Proc. Natl. Acad. Sci. U. S. A. 105 (2008) 18314–18319.
[16] J. Bird, A.J.M. Williams, S.S. Rahman, R.W. Ward, J. Med. Chem. 37 (1994) 158–169.
[17] E. Naydenova, K. Troev, M.T. Ancheva, G. Hagele, I. Ivanov, A. Kril, Amino Acids 33 (2007) 695–702.
[18] M. Collinsova, J. Jiracek, Curr. Med. Chem. 7 (2000) 629–647.
[19] J.D. Compain, P. Mialane, J. Marrot, F. Cheresse, W. Zhu, E. Oldfield, A. Dolbecq, Chem. Eur. J. 16 (2010) 13741–13748.
[20] K.-B. Huang, Z.-F. Chen, Y.-C. Liu, Z.-Q. Li, J.-H. Wei, M. Wang, G.-H. Zhang, Eur. J. Med. Chem. 63 (2013) 76–84.
[21] R.S. Dothager, K.S. Putt, B.J. Allen, B.J. Leslie, V. Nesterenko, P.J. Hergenrother, J. Am. Chem. Soc. 127 (2005) 8686–8696.
[22] V. Nesterenko, K.S. Putt, P.J. Hergenrother, J. Am. Chem. Soc. 125 (2003) 14672–14673.
[23] A. Eastman, Cancer Cells 2 (1990) 275–280.
[24] T. Chen, Y.S. Wong, Int. J. Biochem. Cell Biol. 41 (2009) 666–676.
[25] T. Chen, Y.S. Wong, Cell. Mol. Life Sci. 65 (2008) 2763–2775.
[26] S. Snigdha, E.D. Smith, G.A. Prieto, C.W. Cotman, Neurosci. Bull. 28 (2012) 14–24.
[27] P. Jordana, M.C. Fonseca, Cell. Mol. Life Sci. 57 (2000) 1229–1235.
[28] S. Mahadevan, M. Palaniandavar, Inorg. Chem. 37 (1998) 693–700.
[29] V. Rajendiran, M. Murali, E. Suresh, M. Palaniandavar, V.S. Periasamy, M.A. Akbarsha, Dalton Trans. (2008) 2157–2170.
[30] L. Messori, P. Orioli, C. Tempi, G. Marcon, Biochem. Biophys. Res. Commun. 281 (2001) 352–360.
[31] I. Kraicheva, A. Bogomilova, I. Tsacheva, G. Momekov, K. Troev, Eur. J. Med. Chem. 44 (2009) 3363–3367.
[32] G.M. Sheldrick, SADABS, Version 2.05, University of Göttingen, Göttingen, Germany, 2002.
[33] G.M. Sheldrick, SHELXS-97, Program for Solution of Crystal Structures, University of Göttingen, Göttingen, Germany, 1997.
[34] M.C. Alley, D.A. Scudiero, A. Monks, M.L. Hursey, M.J. Czerwinski, D.L. Fine, B.J. Abbott, J.G. Mayo, R.H. Shoemaker, M.R. Boyd, Cancer Res. 48 (1988) 589–601.
[35] Z.-F. Chen, Y.-F. Shi, Y.-C. Liu, X. Hong, B. Geng, Y. Peng, H. Liang, Inorg. Chem. 51 (2012) 1998–2009.
[36] M.V. Keck, S.J. Lippard, J. Am. Chem. Soc. 114 (1992) 3386–3390.